17th Brazilian Congress of Thermal Sciences and Engineering
November 25th-28th, 2018, Águas de Lindóia, SP, Brazil

ENCIT-2018-0071
ANALYSIS OF WAKE VELOCITIES AND PRESSURE FLUCTUATIONS IN A BISTABLE FLOW USING HILBERT-HUANG TRANSFORM AND WAVELETS

Ana Paula Ost
Roberta Fátima Neumeister
Sérgio Viçosa Möller
Universidade Federal do Rio Grande do Sul. Rua Sarmento Leite, 425 – Porto Alegre/ RS
ana.ost@ufrgs.br
roberta.neumeister@ufrgs.br
svmoller@ufrgs.br

Abstract. *This paper shows the study about pressure fluctuations and velocity results from the wakes of two cylinders side-by-side in a bistable flow. The experimental measurements were conducted in an aerodynamic channel with a pair of 25mm cylinders located in the test section, with a pitch to diameter p/D of 1.26. The tested Reynolds Number is $25.7x10^3$, based on diameter and free stream velocity. The pressure fluctuations were measured using condenser microphones positioned in the upper channel wall and the velocity signals were acquired using hot wire anemometry. In order to perform the analysis of the acquired data, Hilbert-Huang transform is used, as well as continuous wavelet transforms, and PDF (Probability Density Function). The results show the presence of the bistable flow in the raw signal, the PDF shows the changes in the wake modes with the deviation in the pressures occurrences. The continuous wavelet present high energy under 150 Hz and can be associated to the cylinders vortex shedding. Comparing the techniques is observed that Wavelet transform better represents the bistable signals, showing the phenomena and the main frequency ranges. Hilbert-Huang transform shows all the instantaneous frequency modulations present in the signal, the EEMD represents the important oscillations of the flow, and the bistable phenomenon is identified. The Hilbert spectra show the locations of those oscillations on time and amplitude, but the bistable phenomenon is not visible in the spectra.*

Keywords: *Pressure fluctuations, turbulence, Hilbert-Huang transform, Wavelet transform, PDF.*

1. INTRODUCTION

The phenomena of the flow around cylinders is found on a large group of engineering applications like heat exchangers, chimneys, nuclear reactors, pipe lines, with direct influence in project development, particularly as regard the behavior of vortex shedding and fluid-structure interaction. The association of cylinders generates additional phenomena and can amplify the effects in structures (Päidoussis *et al.*, 2011).

When two cylinders of equal diameter placed side-by-side are submitted to a transversal flow, the wake can present peculiar characteristics caused by the interaction of the wakes. The first characteristic observed is a gap flow deviated to the back of one or the other cylinder, this characteristic is present on $p/D < 2$, being D the diameter of the cylinder and p the distance between cylinders center. The second characteristic, consequence of the gap flow deviated, is the formation of two wakes, a narrow wake and a wide wake, presenting distinct velocities and fluctuations. In some cases, the configuration of wake, changes randomly and is called bistable flow. This characteristics are described by (de Paula and Möller, 2013), (Alam et al., 2003), Afgan et al. (2011) and Zhou and Alam (2016).

The flow over cylinders can be analyzed using velocity signals from the wakes and monitoring the pressure. Many studies are observed in the literature as the one presented by Endres and Möller (2001), where the authors experimentally studied the pressure and velocity fluctuations in tube banks with triangular and square arrangements, and four different aspect ratios p/D= 1.60, 1.26, 1.16 and 1.05. They used hot wire anemometry for the velocity fluctuations and a pressure transducer for pressure fluctuations. They concluded that the RMS values of the wall pressure fluctuations scaled with the velocity measured in the center of the narrow gap between the tubes, have approximately the same magnitude for both triangular and square arrays and that they are differently influenced by the gap spacing. For triangular arrangements the lower p/D configurations did not presented a local maximum; only p/D = 1.60 presented a local maximum at 60°. In the square arrays the two largest p/D presented local maxima at 30° and 45°. The reductions in the gap spacing distributed more uniformly the wall pressure fluctuations. Square arrays also presented the same decay pattern after a Strouhal number St = 0.1 in the dimensionless auto spectral densities, this did

not occur in the triangular arrays. Except for the triangular arrangement with *p/D* 1.05, where the highest values of pressure fluctuations were found at 0°, all the other results have almost uniform distributions.

Alam and Zhou, 2007, presented an experimental investigation in the structure of flow using two cylinders alternating the spacing *p/D* = 1.10, 1.13 and 1.20, to understand the physics of each spacing *p/D*. The Authors applied analysis of pressure distributions, the pressure on the surfaces of the cylinders were measured using a pressure transducer and the surface oil technique is employed for flow visualization on the cylinder. Applying those techniques, the authors found that two distinct flow structures occur in *p/D* = 1.10 and 1.20, and, that the lift coefficient shows a sudden change. The spacing flow in *p/D* = 1.10 is highly bistable, forming a clear region of separation in the data. At *p/D* = 1.20 the separation region is much smaller. For the case of *p/D* = 1.13 there are two discontinuous changes in flow structure: one is similar to results for pacing *p/D* = 1.10 and the other to the results for *p/D* = 1.20, presenting thus 4 bistability modes for lift coefficients.

Keogh and Meskell (2015) described the experimental analysis carried out on tubes with triangular arrangement and spacing *p/D* = 1.375. The analysis took into account the pressure obtained on the test section wall and in the wall of two cylinders instrumented with several pressure points. In addition, they used PIV to capture images of the flow. The study covered Re = 0.63×10^4 to Re = 1.27×10^4. The authors verified that in certain flows the pressure signals of each instrumented cylinder present high correlation, they also concluded that at certain speeds the behavior of the pressure changes, resulting in the occurrence of a bistable flow through the tube bank and operates in a three-dimensional arrangement that changes with the flow field mode.

Zhou and Alam (2016) executed a review of previous studies on the wake of two cylinders relating the center-to-center spacing, orientation of the two cylinders with respect to incident flow and Reynolds number. The authors presented the full picture of the flow in terms of a number of regimes. The physical aspects in each regime are discussed, covering the flow structures, Strouhal numbers, pressure distributions, fluid forces, heat and momentum transport characteristics, and Reynolds number effect.

Hilbert-Huang transform (HHT) has found many applications for non-linear and non-stationary data, being applied in many areas of research, i.e. financial analysis (Huang et al., 2003), biological data (Tsai et al., 2016), seismic and geophysics (Battista et al., 2007), among others. There are many examples of applications of HHT in analysis a study of pressure fluctuations: in blood flows (Lo et al., 2008), hydraulic turbines (Wang et al., 2018), hydrofoils (Benramdane et al., 2007), but just a few on pressure fluctuations in turbulent flow.

Debert et al., 2011 applied the Ensemble Empirical Mode Decomposition (EEMD) as a tool for a detailed analysis of time and space characteristics of wall pressure fluctuations in a turbulent flow. The experiment was conducted in an anechoic wind tunnel, and the pressure fluctuations were measured using a linear array of 64 microphones mounted in a flat plate. The EEMD was applied in two experimental configurations. First they measured the wall pressure fluctuations under a turbulent boundary layer flow and analyzed some space time representations of the raw signals, also a wave-frequency analyses was used in order to get a better understanding of the physical content of each IMF mode. Second, they combined artificially the turbulent boundary layer wall pressure data with an airborne diffuse sound field data, and then performed the EEMD analysis for signals containing both acoustic and hydrodynamic phenomena. For the first set of data the EEMD proved to be an efficient tool, they observed some merging and splitting phenomena, which could be highlighted when considering specific IMFs, however, the acoustic energy produced by the turbulent boundary layer was not detected in the data. For the second set of data, the observed that the low-order IMF capture the small-scale hydrodynamic fluctuations, high-order IMF mainly capture the large-scale acoustic fluctuations and the residue predominates the acoustic fluctuations. Therefore EEMD is an efficient tool for performing the separation of hydrodynamic and acoustic phenomena that are potentially present in experimental data.

(Meng et al., 2012) studied the features of turbulent flow in a Kenics Static Mixer (KMS) using the Hilbert-Huang transform, based on the Empirical Mode Decomposition (EMD). They used 6 pressure transducers installed on different positions on the walls of the mixer to measure the gauge pressure fluctuations. The medium was deionized water and the measurements were made at a range of different Reynolds numbers (Re = 1756~3512) considered to be in turbulent flow regimes in KSM. They also analyzed the pressure fluctuations under different axial and radial positions. They concluded that Hilbert spectral analysis shows the variations in the pressure fluctuations, identifying the maximum energy and the vortex scales, as well as the largest pulsation amplitudes, being a good tool to describe the flow behavior.

The purpose of the present study is to analyze the features of the wake velocities and corresponding pressure fluctuations in a bistable flow after two cylinders side-by-side with *p/D* = 1.26, with non-ergodic signals. The analysis applies the Hilbert spectral analysis based on EEMD, Probability Density Functions (PDFs), Continuous Wavelets and Fourier transform and aims to investigate the principal characteristics observed with each technique applied.

2. METHODOLOGY

Pressure fluctuations result from velocity fluctuations on several points of the flow flied. The Poisson's equation describes the resulting pressure field, obtained from de divergent of Navier-Stokes equation (Endres and Möller, 2001)

$$\nabla^2 p' = -\rho \frac{\partial^2 (u_i u_j)}{\partial x_i \partial x_j}. \tag{1}$$

Introducing Reynolds statement in Eq. 01, representing velocity components and pressure by their time average value and fluctuating part, the equation can be rewritten in terms of pressure fluctuation

$$\nabla^2 p' = -2\rho \frac{\partial \overline{u_i}}{\partial x_j} \frac{\partial u'}{\partial x_i} - \rho \frac{\partial^2 (u_i' u_j')}{\partial x_i \partial x_j} + \rho \frac{\partial^2 \overline{u_i' u_j'}}{\partial x_i \partial x_j}. \tag{2}$$

Pressure fluctuations are produced by the interaction of velocity gradients with velocity fluctuations and Reynolds stresses (Rotta, 1972). According to Townsend (1976), the amplitude of the pressure fluctuations may be influenced by velocity fluctuations at a distance comparable with the wavelength of these fluctuations. The search of form and magnitude of pressure and velocity fluctuations, and the interdependence between these quantities are necessary for the comprehension of the phenomena described in this paper.

In the present study the pressure and velocity signals are analyzed applying statistics moments, as described in Tennekes e Lumley (1972), where de first moment is zero because is the temporal mean of fluctuations. The second moment is the variance that is the root mean square of the fluctuations. The third moment represents the asymmetry of the signal and the fourth moment indicates the flatness of the signal. The cross-correlation also is applied for two signals and indicates the relation between the signals.

The Fourier Transform is the approximation of the temporal signal using sines an cosines sums, this process allow the identification of the main frequencies in the signal (Tennekes e Lumley, 1972). The present study applied Fourier Transform using the pressure and velocity fluctuations as Endres and Möller (2001).

The Fourier Transform indicates the main frequencies in the signal, but it does not show the time that the frequency is present and how signals from bistable flows are non-ergodic the application of wavelets is important. The wavelets show the characteristics in one window time-frequency. A wavelet function is necessary for the analysis and in the present study the Db20 is applied, this function characterizes turbulent signals, as detailed in Indrusiak (2004); Indrusiak *et al*. (2005). The signals were detailed and analyzed applying wavelet continuous spectrum using wavelet Db 20 on the frequency range of 1 to 800 Hz with divisions of 3Hz.

Hilbert-Huang transform is a combination of the Empirical Mode Decomposition (EMD) and the Hilbert Spectral Analysis (HSA) that enables the treatment of non-linear and non-stationary data (Huang et al., 1998). The EMD is a direct and adaptive method, with a posteriori-defined basis derived from the data (Huang and Shen, 2005). The method identifies the intrinsic oscillatory modes by their characteristic time scales in the data; each of these oscillatory modes is represented by an intrinsic mode function (IMF). IMF is a function that satisfies two conditions: (1) the number of extrema and the number of zero crossings must either equal or differ at most by one; and (2) at any point, the mean value of the envelope defined by the local maxima and local minima envelopes, is zero.

The decomposition follows the assumptions determined by (Huang et al., 1998): i) the signal has at least two extrema, a maximum and a minimum; ii) the characteristic time scale is defined by the time lapse between the extrema; iii) if the data were totally devoid of extrema but contained only inflection points, it can be differentiated one or more times to reveal the extrema. The steps involved in the EMD decomposition are describe by many authors, like, (Huang et al., 1998, Huang and Shen, 2005; Huang and Wu, 2008; Rilling and Flandrin, 2008); among others.

The decomposed data can be written in terms of Intrinsic Mode Functions as

$$x(t) = \sum_{j=1}^{n} c_i(t) + r_n(t) \tag{3}$$

where $c_i(t)$ are the IMF modes and $r_n(t)$ is a residue, or trend, which is a monotonic function or has at most one extreme point. Several stopping criteria for the sifting process were developed to avoid over-sifting and guarantee that the intrinsic mode functions retain the physical sense; herein the standard deviation criterion is adopted (Huang et al., 1998). Because of the dyadic filter bank property of the EMD, for an N data length, the finite number of steps in the decomposition satisfies the relation $n \leq \log_2 N$ (Flandrin et al., 2004; Wu and Huang, 2004).

However EMD has some problems, like the frequent appearance of mode mixing, which is usually a consequence of signal intermittency. To overcome the mixing mode problem and properly separate the scales, a noise-assisted data analysis method was used, called the Ensemble Empirical Mode Decomposition (EEMD). The method is based on studies of statistical properties of white noise (Wu and Huang, 2004; Wu and Huang, 2009; Tsui et al., 2010; Yeh et al., 2010).

A joint probability distribution, defines the simultaneous behavior of two random variables, the mathematical details can be found in (Pope, 1985; Pope, 2000; Montgomery and Runger, 2002 and Haworth, 2010). The PDF (Probability Density Function) displays the number of occurrences relating two or more random variables, in the present analysis two variables are related. The PDFs displays the bins as 3-D rectangular bars, and the height of each bar indicates the number of elements of the bins related to pressure and velocity signals in study, representing the occurrences of time, pressure fluctuations and velocity.

3. TEST SECTION AND MEASUREMENT TECHNIQUE

The aerodynamic channel used in the experiments, shown in Fig. 1 (a), is made of acrylic glass, with a rectangular test section of 0.146 m height, width of 0.193 m and 0.9 m length. The airflow is driven by a centrifugal fan with 1HP, and passes through two honeycombs and two screens, to reduce the turbulence intensity to about 1% of the free stream velocity in the test section. Upstream the test section, placed in one of the sidewalls, a Pitot tube measures the reference velocity of the impinging flow, and this is considered as the average velocity in the channel.

Condenser microphones with 1/8" diameter (Brüel & Kjaer, Type 4138) flush-mounted with the channel walls in the wake region behind the cylinders are applied for the measurements of the wall pressure fluctuations. The microphones assembly includes pre-amplifier, conditioner, and an energy source. The output signal in volts is acquired with an A/D 16 bits board, model NI USB-9162, with four channels. The microphones are positioned in the cylinders wakes, as shown in Fig. 1 (b), with fixed location in the aerodynamic channel top wall. The cylinders with diameter of 25mm are fixed in the position 0.69 m from the last channel screen, with *p/D* 1.26. The Reynolds number, based on the free stream velocity and cylinder diameter, is 25.7×10^3. The acquisitions were executed with frequency of 3 kHz and the associated error is around 5%. The velocity values from the wake were obtained by hot wire anemometry technique applying two single wire probes (55P11) in the positions presented in Fig. 1 (c), Streamline DANTEC, with acquisition frequency of 3 kHz. The pressure and velocity acquisitions were executed simultaneously. The uncertainties of the measurements are about 3% in the velocity.

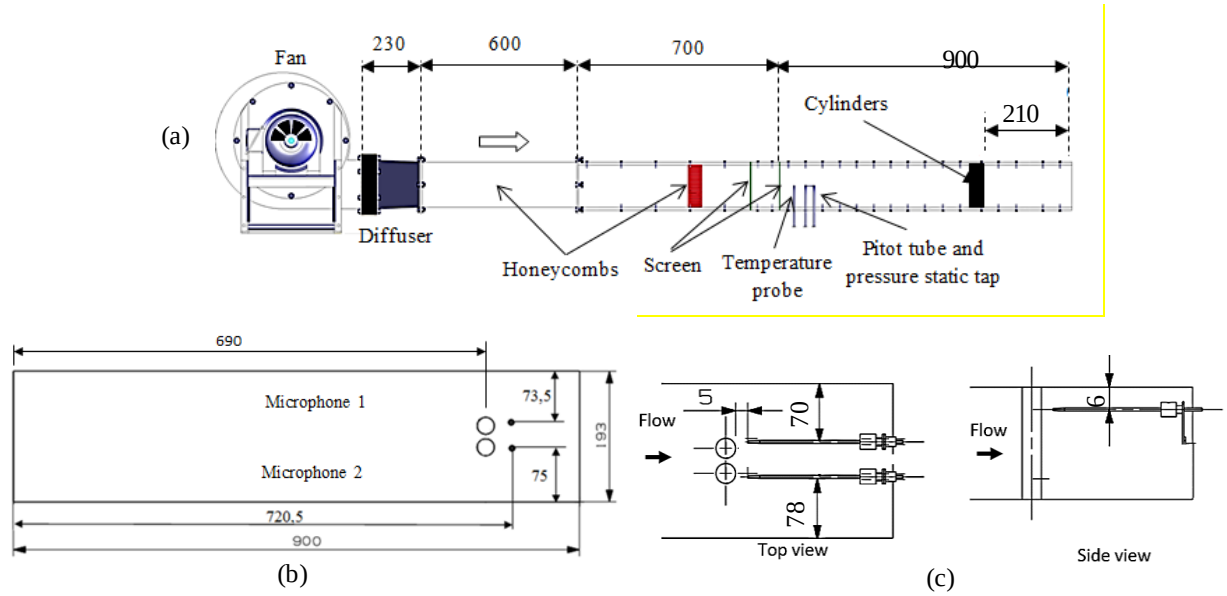

Figure 1. Schematic view of (a) the aerodynamic channel, (b) the condenser microphones positions and (c) hot wire probe positions.

4. RESULTS AND DISCUSSIONS

The pressure fluctuation and velocity time series, for a bistable flow after two parallel cylinders, with pitch to diameter *p/D* = 1.26, are illustrated in Fig. 2. The bistability is seen in the pressure fluctuations, the large amplitudes correspond to the narrow wake, while the small amplitudes correspond to the wide wake. The velocity results show the modes differences with velocity mean values higher for the narrow wake and smaller for the wide wake.

The statistic characteristics of each signal are presented in Table 1, where the minimum and maximum values are observed and present similar values for the velocity but, a significant difference between the pressure results, this difference may be referent to the position of the microphones and the wake characteristic. The variance is higher in pressure signals, due to the magnitude of the fluctuations; in the velocity results U1 presents higher fluctuations, another factor of influence is the duration of each bistable mode. The third moment, or skewness, represents the signal

asymmetry, with total symmetry when the parameter is zero. The signal P1 presents higher symmetry than P2 and the same relation is observed between U1 e U2; this behavior can be related to the wake modes in each signal. The results of kurtosis indicate that the signal U1 is the most concentrated while the other signals are more disperse.

Figure 3 presents the cross-correlation function for pressure and velocity signals. In Fig. 3 (a) the coefficient represents the relation for U1 and U2, a correlation coefficient around 0.7 is observed, indicating a strong correlation and equivalence between the signals; with crescent time, the number of points to relate between the signals reduces and the correlation coefficient decreases. The cross-correlation from for pressure P2 and velocity U2 in Fig. 3 (b), presents low coefficients due to the different positions where the signals are acquired, the velocity data is obtained from the wake after the cylinder in 6mm from the top wall, as indicated in Fig. 1 (c), and the pressure from the channel top wall. This distance might not allow high influence from one to another. The effects of the measurement position are also visible in the cross-correlation for both pressures, Fig. 3(c), where the coefficient presents a maximum value around 0.28 indicating a low correlation and decreases along time.

Table 1. Statistic characteristics of each signal

	P1 [Pa]	P2 [Pa]	U1 [m/s]	U2 [m/s]
Minimum	-108,69	-224,22	0,349	0,282
Maximun	74,42	111,28	27,8	28,4
Second Moment -Variance	129,13	508,23	23,48	11,39
Third Moment - Skewness	-0,092	-0,21	0,174	1,067
Fourth Moment - Kurtosis	4,934	5,89	2,198	4,463

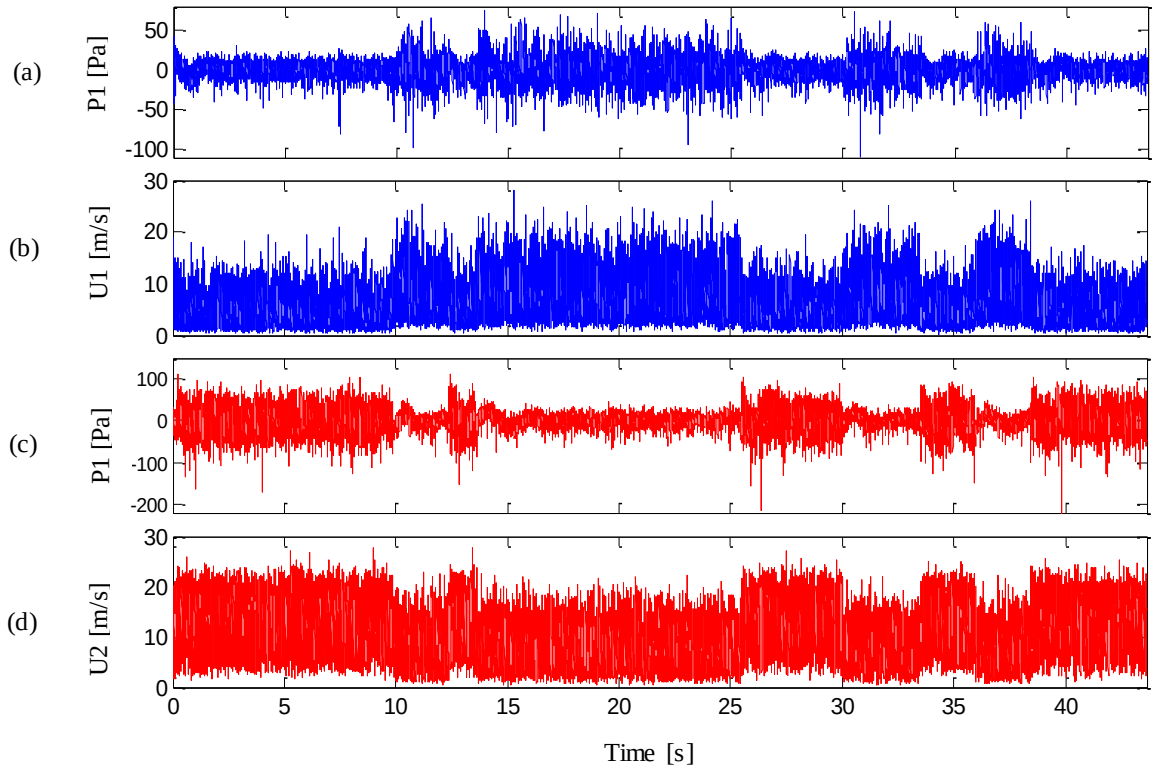

Figure 2. Velocity signals and pressure fluctuations for, (a) microphone 1 (P1), (b) probe 1 (U1), (c) microphone 2 (P2) and (d) probe 2 (U2).

The power spectrums of the wall-pressures and velocity are seen in Fig. 4. For both pressure data, P1 and P2, Fig. 4 (a), it is possible to observe the presence one main frequency at 79.1 Hz that corresponds to the vortex shedding frequency. This frequency generates a Strouhal number ($St = fD/U$) of 0.126 and is similar to the results showed in Blevins (1990) and Alam et al. (2003), for cases with two cylinders side-by-side with small p/D. The power spectrum for velocities signal is presented in Fig. 4 (c) and for both signals a small peak in 79.1Hz is visible. The higher frequencies observed in the pressure spectrum may be related to the microphone cover and to the wall alignment, once that the cover do not present linear shape. The cover and position can generate noise in the spectrum and present a behavior that differs from the velocity results.

In the power spectrum, P2 presents higher amplitudes of energy. In addition to the characteristic peaks of the flow, the spectra also present various narrow peaks. Running out the difference between P2 and P1, the frequency peak corresponding to the vortex shedding is magnified, and lies in the same frequency as in the velocity spectra, the other peaks disappear because they have the same phase and intensity and are likely produced by resonances of the test section. A similar result was found in tube bundles by (Möller, 1991).

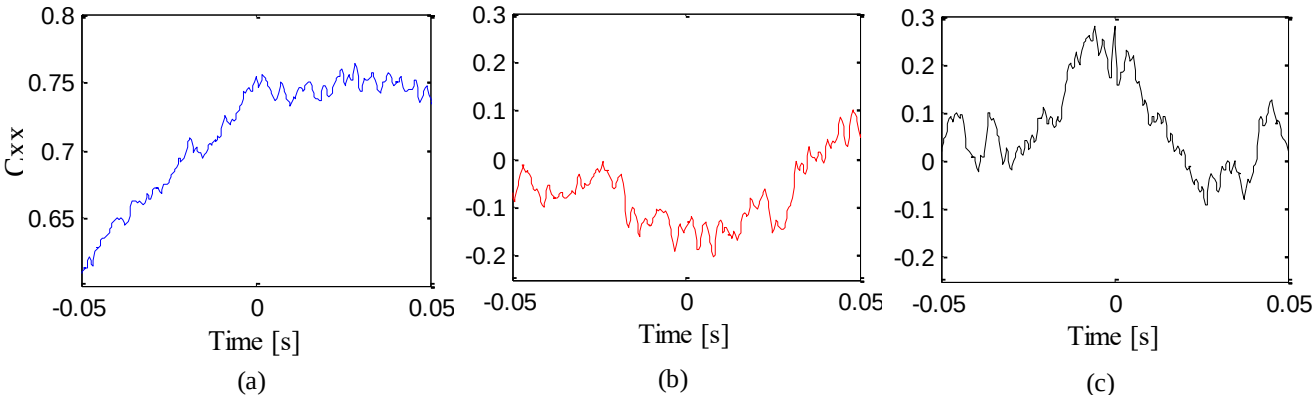

Figure 3. (a) Cross-correlation U1U2, (b) .Cross-correlation P2U2 and (c) cross-correlation P1P2.

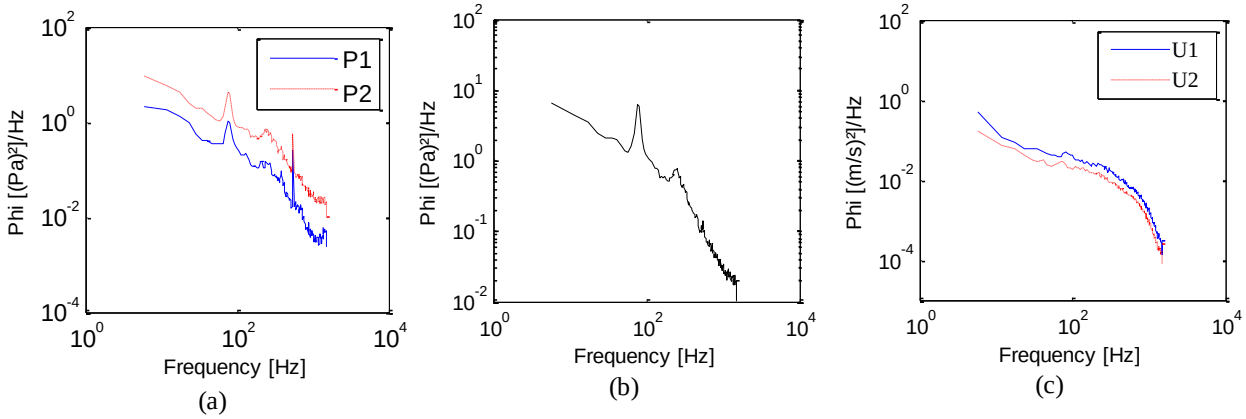

Figure 4. Fourier spectra analysis of (a) the pressure fluctuations P1 and P2; (b) the difference between P2 and P1 and (c) velocity fluctuations U1 and U2.

The Ensemble empirical mode decomposition (EEMD) is applied on the wall pressure fluctuations and velocity signals. For all sets of data the decomposition generated 16 IMFs and a trend, which is monotonic function from which no IMF can be further extracted. Figure 5 shows a 15 seconds fragment of the first eighth IMF components for pressure signal P1 and velocity U1, this time interval corresponds to two mode switching in the flow wake. It is also possible to identify on the IMF the bistable behavior in the oscillations between IMF C3 and C8, higher orders IMF do not present the bistable characteristics.

The IMF components tend to organize as a filter bank structure, essentially the first mode (C1) is a high pass filter, and the higher orders IMF are characterized by a set of overlapping bandpass filters. Consequently, the IMFs are distributed from high frequency to low frequency, so the first (C1) contains information with respect to the inertial subrange, or the smaller scale measured, IMF C2 to C5 contain the wave modulations of the energy containing range, IMF C6 to C8 represent the large scales in the flow, contributing to the fluid motion energy and are related to the vortices generated by the channel itself. The higher orders IMF do not contribute significantly with energy to the fluid motion and are omitted in this study.

The IMFs were than processed by Hilbert transform, and the Hilbert spectra are showed in Fig. 6. The Hilbert spectral analysis shows the instantaneous frequency at each corresponding time and energy amplitude, it can be interpreted as a weighted non-normalized joint amplitude-frequency-time distribution, showing the exact occurrence time of each flow oscillation. As can be seen most of the energy of pressure signals is concentrated in frequencies lower than 20 Hz, this effect is caused by the decomposition process, that creates a number of pseudo-frequencies in the low frequency range that have no physical significance or energy contribution to the fluid motion. The important IMF components containing information about the flow scales are the ones amidst C1 and C8. Those components consist of the higher frequencies and the HSA fails in representing them properly in respect to the signal characteristics and the

occurrence of frequencies far apart in the same oscillation. Notwithstanding one can see a concentration of energy on the range of the vortex shedding frequency around 79.1 Hz and in ranges that agree with the presence of a first (158 Hz) and second (316 Hz) harmonics, even if dispersed. The bistable phenomenon is not identified in the HSA, since it only represents the fluid oscillations located in time and amplitude, not the phenomenon itself.

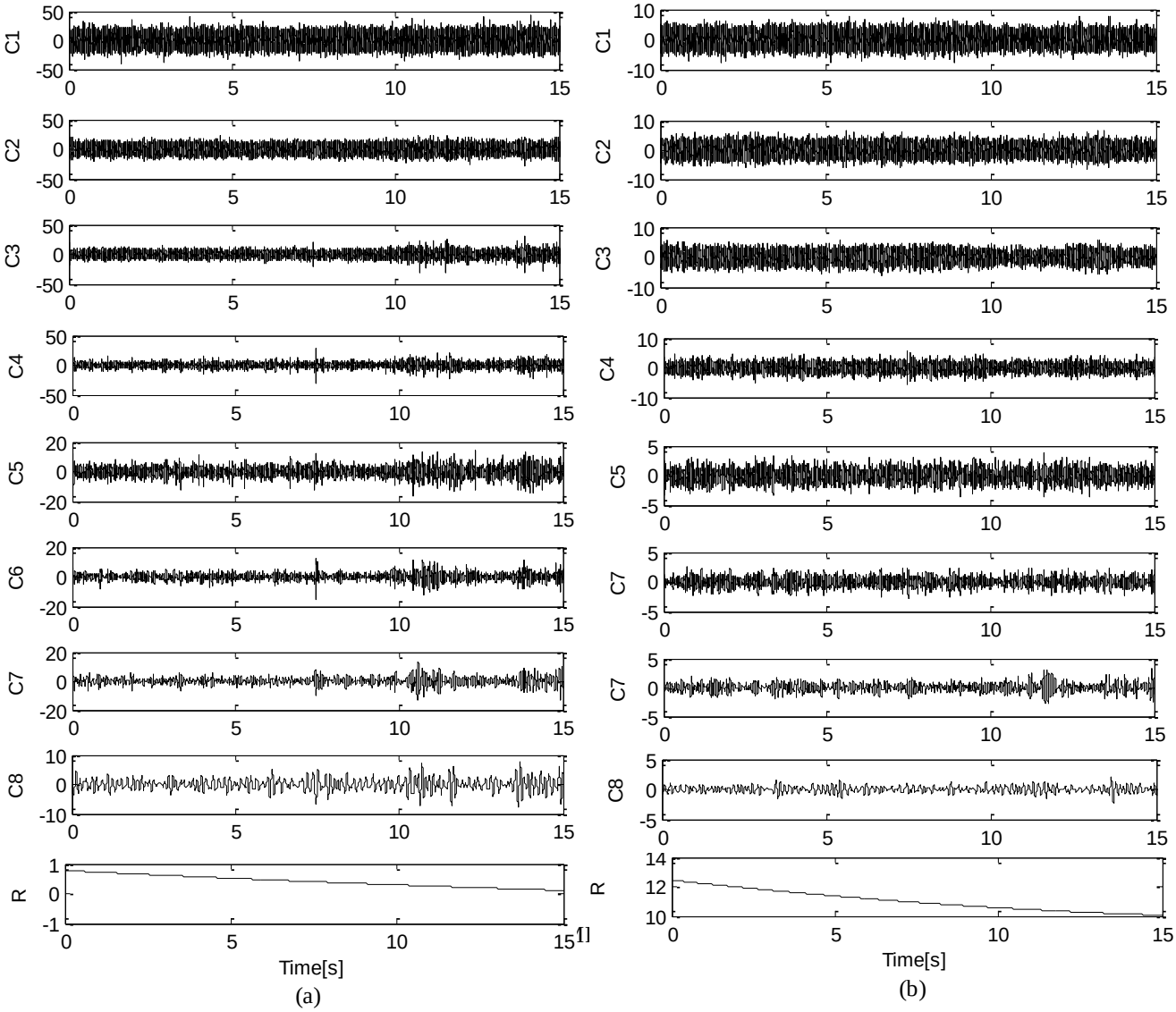

Figure 5. IMF components (C1 to C8) and residue (R) for (a) pressure fluctuations P1 and (b) velocity signal U1.

The continuous wavelet spectrum shows the energy distribution in frequency ranges along time. The velocity and pressure behavior relating time, frequency and energy intensity are observed at the Figure 7. The wavelet analysis is executed with the wavelet function dB20, using increase of 3Hz and upper limit of 800Hz.

Analyzing the continuous wavelet spectrum for P1, Fig. 7 (a), it is observed that the energy levels reach frequencies around 500 Hz for the narrow wake. For the wide wake, the energy levels are about 100 Hz, reach until 200 Hz in some regions. In the signal from P2, Fig. 7 (b), the energy levels are higher than for P1, showing the wide wake with energy less than 200 Hz but with some peaks at higher frequencies. The narrow wake shows high values of energy, up to 500 Hz and peaks of energy at higher frequencies in a few moments, this is probably caused by the characteristic of stretching and contracting the wave which causes a distortion on frequencies higher than 500 Hz. The presence of the bistable flow is clear comparing the results in both cases and the high energy observed in P2 is related to the pressure values on the signal that can be caused by the positions of the microphones.

Figure 7 (c) presents the wavelet spectrum from the velocity signals and it is visible that the energy levels are lower than the ones from the pressure signals, but the same phenomenon is observed. Presents lower energy during some periods, representing the wide wake, and higher energy in other periods, represents the narrow wake. The same

characteristics are observed in Fig. 7(d) for U2, but with opposite energies due the bistable characteristic of the flow represented in the signal.

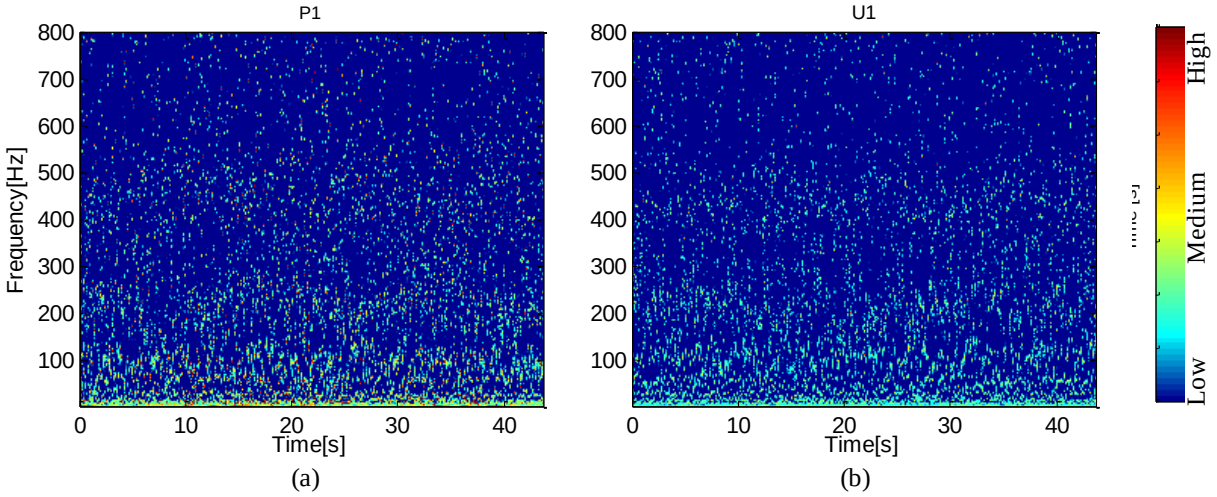

Figure 6. Hilbert Spectrum for the IMFs of (a) pressure fluctuation P1, and (b) velocity U1.

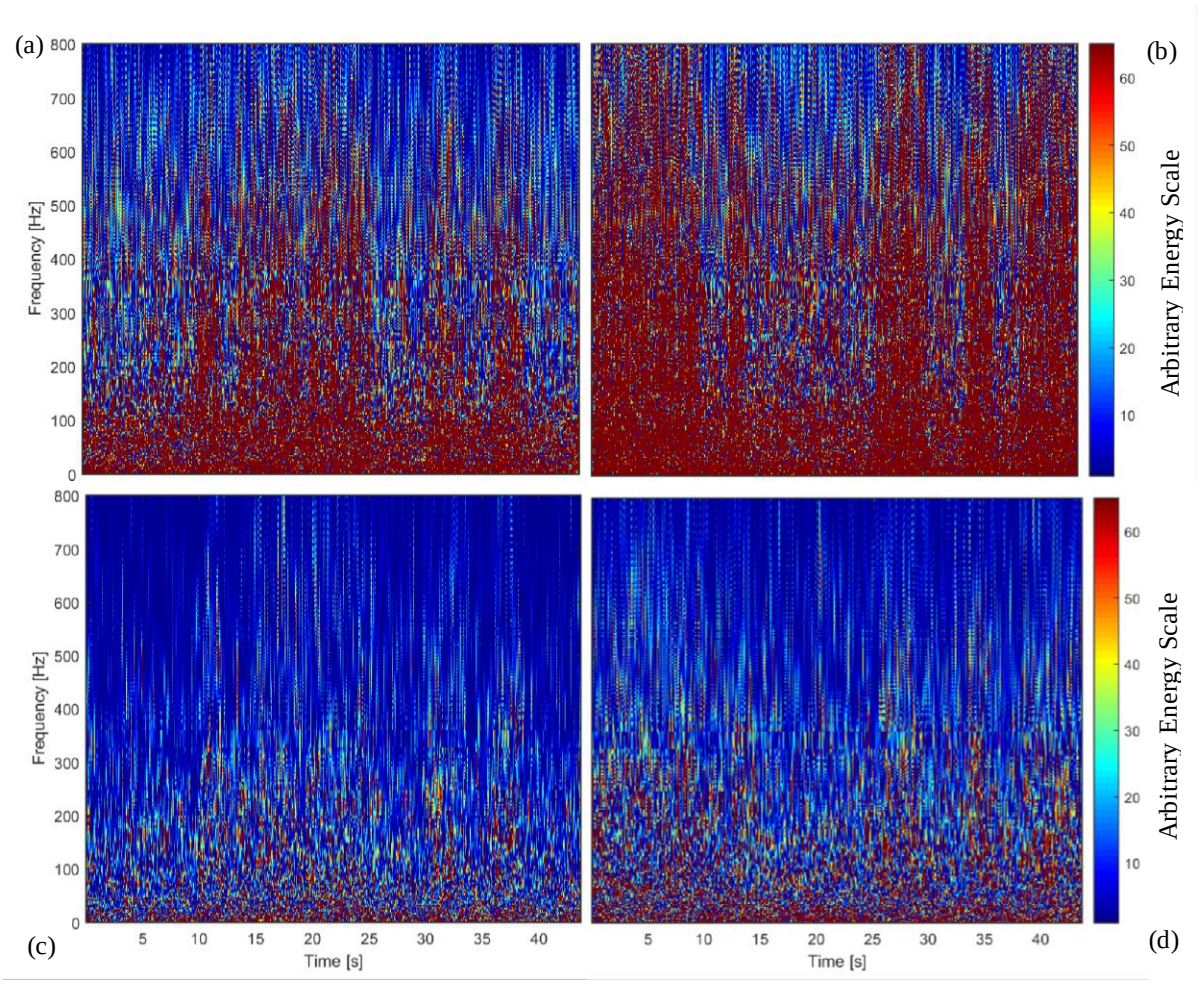

Figure 7. Continuous wavelet from pressure signal a) P1, b) P2, c) U1 and d) U2

Figure 8 presents the bivariate histograms using equally spaced bins, where the z-axes represents the number of occurrences and two variables were related in the x and y-axes. Figure 8 (a) presents the number of occurrences of pressure P1 in time, with the representation of the raw signal and clear representation of wake modes. From the signal U1, Fig. 8 (b), the occurrences present higher concentration near the mean of each mode and indicating each mode

clearer than in the raw signals presented in Fig. 2. The relation between the signals of pressure and velocity are presented in Fig. 8 (c), where the wake modes are not visible and the concentration is in the intersection of the each signal mean, zero for the pressure and eleven for the velocity.

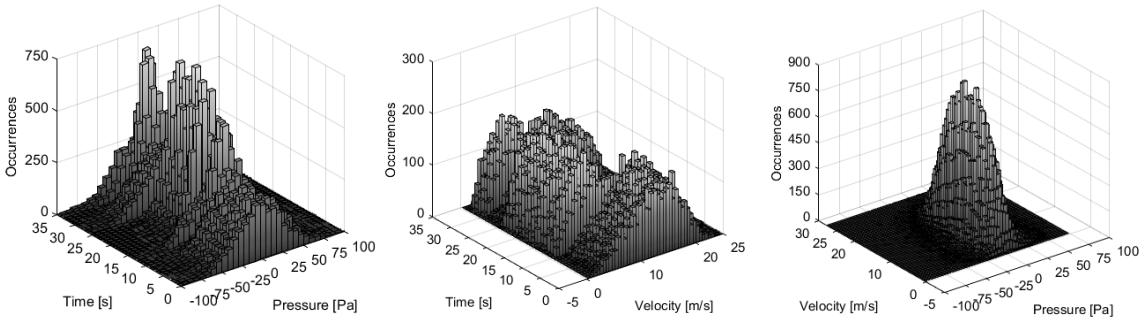

(a) (b) (c)

Figure 8. 3D bivariate histogram for (a) P1×time, (b) U1×time and (c) P1×U1.

5. CONCLUSIONS

The study presented an analyzes of the features of the wake velocity and pressure fluctuations for a bistable flow after two cylinders side-by-side with p/D = 1.26, with the objective to compare the techniques of Hilbert spectral analysis based on EEMD, PDF, Wavelets and Fourier transform.

The results show that the statistics moments are highly affected by the bistable flow, the non-ergodic signal generates significant changes because of the acquisition positions. The correlation coefficient is high between velocities due the coefficients around 0.7, the pressure results indicate low correlation an even lower correlation is observed for the pressure and velocity signals. The low correlation for the pressure and velocity signals can be caused by the positions of probes and microphones, where microphones are in the wall.

The analysis using Fourier transform indicates the main frequencies related to the phenomena, but do not indicate the presence of the bistability. The pressure results bring levels of energy in the peaks of frequency higher than the velocity, although in the pressure signals there are presence of noise due the cover and the wall proximity.

The EEMD provided a clear identification of the flow modulations containing the bistable phenomenon; those frequency modulations were located mainly from IMF C3 to IMF C8. The higher orders IMF are considered pseudo-frequencies generated by the decomposition method and do not contribute energetically with the fluid motion.

The Hilbert spectral analysis represents the energy distribution on the time and frequency. As a characteristic of the method, it decomposes the data in IMF, each one containing the instantaneous frequencies of the data. Since bistable phenomenon occurs in a wide range of frequencies and amplitudes simultaneously, the same IMF can contain more than one frequency at a time, consequently the energy representation of the spectrum becomes disperse and the frequency ranges not clearly distinguishable. Although one can see that the energy tends to concentrates around frequencies that correspond to the vortex shedding and its harmonics.

Continuous Wavelet transform results show the bistable phenomena in clear levels of energy and, as in the transform Fourier results, the energy magnitude is significantly higher in the pressure signals. This characteristic is a result of to the variable magnitude, once the pressure fluctuations are higher than the velocity fluctuations. The wavelet transform also allow the observation of the main frequencies associated to each signal and in each wake mode of the bistable behavior. On the other hand, the wavelet characteristic can distort the signal vertically, and the phenomenon influence can be seen in higher frequencies than the ones it actually occurs. Wavelet transform give a uniform frequency resolution, consequently time resolution, is also, uniformly poor.

The PDF results show the bistable flow if one of the random variables is the time, with clear characteristic than the raw signal. If the PDF analysis englobe pressure and velocity the observation is the concentration region, that englobe both signals mean value and do not indicate the bistable phenomena.

This study demonstrated the differences and potential results that can be obtained using different analysis methods. Wavelet transform appears to be the technique that represents qualitatively the bistable phenomena with more accuracy, while Hilbert-Huang transform describes the flow features, allowing the identification of flow scales, instantaneous frequencies and amplitudes, and the recognition of flow properties that other tools may neglect or imprecise. The combination of more than one method may contribute to the description of turbulent bistable flows.

6. ACKNOWLEDGEMENTS

This research work was partially supported by CNPq, National Council for Scientific and Technological Development, Ministry of Science, Technology and Innovation, Brazil.

B & K equipment were donated by KIT – Karlsruhe Institut für Technologie, Germany. Authors are gratefully indebted to Dr. L. Meyer.

Roberta Neumeister thanks CAPES, Ministry of Education for granting her a Fellowship.

7. REFERENCES

Alam, M.M., Moriya, M., Sakamoto, H., 2003. Aerodynamic characteristics of two side-by-side circular cylinders and application of wavelet analysis on the switching phenomenon. *J. Fluids Structures*, v.18, p. 325–346.

Alam, M. M.; Zhou, Y. 2007. Flow around two side-by-side closely spaced circular cylinders. *Journal of Fluids and Structures*, v. 23, n. 5, p. 799–805.

Afgan, I.; Kahil, Y.; Benhamadouche, S.; Sagaut, P. 2011. Large eddy simulation of the flow around single and two side-by-side cylinders at subcritical Reynolds number, *Physics of Fluids*, v. 23, n. 17, p. 075101.

Battista, B., Knapp, C., McGee, T., Goebel, V., 2007. Application of the empirical mode decomposition and Hilbert-Huang transform to seismic reflection data. *Geophysics*, v. 72, p. H29–H37.

Benramdane, S., Cexus, J.-C., O. Boudraa, A., Astolfi, J., 2007. Time-Frequency Analysis of Pressure Fluctuations on a Hydrofoil Undergoing a Transient Pitching Motion Using Hilbert-Huang and Teager-Huang Transforms.

de Paula, A.V., Möller, S.V., 2013. Experimental study of the bistability in the wake behind three cylinders in triangular arrangement. *J. Braz. Soc. Mech. Sci. Eng*.

Debert, S., Pachebat, M., Valeau, V., Gervais, Y., 2011. Ensemble-Empirical-Mode-Decomposition method for instantaneous spatial-multi-scale decomposition of wall-pressure fluctuations under a turbulent flow. *Exp. Fluids*, v. 50, p. 339–350.

Endres, L.A.M., Möller, S.V., 2001. On the fluctuating wall pressure field in tube banks. *Nucl. Eng. Des.* 203, 13–26.

Flandrin, P., Rilling, G., Goncalves, P., 2004. Empirical mode decomposition as a filter bank. *IEEE Signal Process. Lett*, v. 11, p. 112–114.

Haworth, D.C., 2010. Progress in probability density function methods for turbulent reacting flows. *Prog. Energy Combust. Sci*., v. 36, p. 168–259.

Huang, N.E., Shen, S.S., 2005. **Hilbert-Huang Transform and Its Applications**. World Scientific.

Huang, N.E., Shen, Z., Long, S.R., Wu, M.C., Shih, H.H., Zheng, Q., Yen, N.-C., Tung, C.C., Liu, H.H., 1998. The empirical mode decomposition and the Hilbert spectrum for nonlinear and non-stationary time series analysis. *Proc. R. Soc. Lond. Math. Phys. Eng. Sci*., v. 454, p. 903–995.

Huang, N.E., Wu, M.-L., Qu, W., Long, S.R., Shen, S.S.P., 2003. Applications of Hilbert–Huang transform to non-stationary financial time series analysis. *Appl. Stoch. Models Bus. Ind*., v. 19, p. 245–268.

Huang, N.E., Wu, Z., 2008. A review on Hilbert-Huang transform: Method and its applications to geophysical studies. *Rev. Geophys*., v. 46, RG2006.

Indrusiak, M.L.S., 2004. Caracterização de escoamentos turbulentos transientes usando a transformada de ondaletas.

Indrusiak, M. L. S.; Goulart, J. V.; Olinto, C. R.; MÖLLER, S. V. Wavelet time–frequency analysis of accelerating and decelerating flows in a tube bank. *Nuclear Engineering and Design*, v. 235, n. 17–19, p. 1875–1887, 2005.

Lo, M.-T., Hu, K., Liu, Y., Peng, C.-K., Novak, V., 2008. Multimodal Pressure-Flow Analysis: Application of Hilbert Huang Transform in Cerebral Blood Flow Regulation. EURASIP J. Adv. Signal Process. 2008, 785243.

Meng, H., Liu, Z., Yu, Y., Wu, J., 2012. Time-frequency analysis of Hilbert spectrum of pressure fluctuation time series in a Kenics Static Mixer based on empirical mode decomposition. *Braz. J. Chem. Eng*., v.29, p. 167–182.

Möller, S.V., 1991. On Phenomena of Turbulent Flow Through Rod Bundles. *Exp. Therm. Fluid Sci*., v. 4, p. 25–35.

Montgomery, D.C., Runger, G.C., 2002. **Applied Statistics and Probability for Engineers**, 3rd ed. John Wiley & Sons.

Pope, S.B., 2000. **Turbulent Flows**. Cambridge University Press.

Pope, S.B., 1985. PDF methods for turbulent reactive flows. *Prog. Energy Combust. Sci*., v. 11, p. 119–192.

Rilling, G., Flandrin, P., 2008. One or Two Frequencies? The Empirical Mode Decomposition Answers. *IEEE Trans. Signal Process*, v. 56, p. 85–95.

Tennekes, H.; Lumley, J. L. **A First Course in Turbulence**. MIT Press, Massachusetts, 1972.

Tsai, F.-F., Fan, S.-Z., Lin, Y.-S., Huang, N.E., Yeh, J.-R., 2016. Investigating Power Density and the Degree of Nonlinearity in Intrinsic Components of Anesthesia EEG by the Hilbert-Huang Transform: An Example Using Ketamine and Alfentanil. PLOS ONE 11, e0168108.

Tsui, P.-H., Chang, C.-C., Huang, N.E., 2010. Noise-modulated empirical mode decomposition. *Adv. Adapt. Data Anal*. v. 02, p. 25–37.

Townsend, A.A., 1976. **The Structure of Turbulent Shear Flow**. Cambridge University Press, Cambridge, UK.

Wang, W., Chen, Q., Liang, X., Yue, X., Dou, J., 2018. A Novel Multidimensional Frequency Band Energy Ratio Analysis Method for the Pressure Fluctuation of Francis Turbine. *Math. Probl. Eng*.

Wu, Z., Huang, N.E., 2009. Ensemble empirical mode decomposition: a noise-assisted data analysis method. *Adv. Adapt. Data Anal*. v. 01, p.1–41.

Wu, Z., Huang, N.E., 2004. A study of the characteristics of white noise using the empirical mode decomposition method. *Proc. R. Soc. Lond. Math. Phys. Eng. Sci*. v. 460, p. 1597–1611.

Yeh, J.-R., Shieh, J.-S., Huang, N.E., 2010. Complementary ensemble empirical mode decomposition: a novel noise enhanced data analysis method. *Adv. Adapt. Data Anal*. v. 02, p. 135–156.

Rotta, J.C., 1972. **Turbulente Strömungen**. B.G. Teubner, Stuttgart.

Päidoussis, M. P., Price, S. J. e de Langre, E. 2011. **Fluid-Structure Interactions: Crossflow-Induced Instabilities**. Cambridge University Press, Nova Iorque.

Zhou, Y. e Alam, M. M. 2016. Wake of two interacting circular cylinders: A review. *Int. J. Heat Fluid Flow*. v. 62, Part B., p. 510-537.

8. RESPONSIBILITY NOTICE

The authors are the only responsible for the printed material included in this paper.